

1 **Dead zone or oasis in the open ocean? Zooplankton**
2 **distribution and migration in low-oxygen modewater**
3 **eddies**

4

5 **Helena Hauss¹, Svenja Christiansen¹, Florian Schütte¹, Rainer Kiko¹, Miryam**
6 **Edvam Lima², Elizandro Rodrigues², Johannes Karstensen¹, Carolin R.**
7 **Löscher^{1,3}, Arne Körtzinger^{1,4} and Björn Fiedler¹**

8 [1]{GEOMAR Helmholtz Centre for Ocean Research Kiel, Düsternbrooker Weg 20, 24105
9 Kiel, Germany}

10 [2]{Instituto Nacional de Desenvolvimento das Pescas (INDP), Cova de Inglesa, Mindelo,
11 São Vicente, Cabo Verde}

12 [3]{Institute for General Microbiology, Kiel, Germany}

13 [4]{Christian Albrecht University Kiel, Kiel, Germany}

14

15 Correspondence to: H. Hauss (hhauss@geomar.de)

16

17 **Abstract**

18 The eastern tropical North Atlantic (ETNA) features a mesopelagic oxygen minimum zone
19 (OMZ) at approximately 300-600 m depth. Here, oxygen concentrations rarely fall below 40
20 $\mu\text{mol O}_2 \text{ kg}^{-1}$, but are expected to decline under future projections of global warming. The
21 recent discovery of mesoscale eddies that harbour a shallow suboxic ($<5 \mu\text{mol O}_2 \text{ kg}^{-1}$) OMZ
22 just below the mixed layer could serve to identify zooplankton groups that may be negatively
23 or positively affected by on-going ocean deoxygenation. In spring 2014, a detailed survey of a
24 suboxic anticyclonic modewater eddy (ACME) was carried out near the Cape Verde Ocean
25 Observatory (CVOO), combining acoustic and optical profiling methods with stratified
26 multinet hauls and hydrography. The multinet data revealed that the eddy was characterized
27 by an approximately 1.5-fold increase in total area-integrated zooplankton abundance. At
28 nighttime, when a large proportion of acoustic scatterers is ascending into the upper 150 m, a

29 drastic reduction in mean volume backscattering (S_v , shipboard ADCP, 75kHz) within the
30 shallow OMZ of the eddy was evident compared to the nighttime distribution outside the
31 eddy. Acoustic scatterers were avoiding the depth range between about 85 to 120 m, where
32 oxygen concentrations were lower than approximately $20 \mu\text{mol O}_2 \text{ kg}^{-1}$, indicating habitat
33 compression to the oxygenated surface layer. This observation is confirmed by time-series
34 observations of a moored ADCP (upward looking, 300kHz) during an ACME transit at the
35 CVOO mooring in 2010. Nevertheless, part of the diurnal vertical migration (DVM) from the
36 surface layer to the mesopelagic continued through the shallow OMZ. Based upon vertically
37 stratified multinet hauls, Underwater Vision Profiler (UVP5) and ADCP data, four strategies
38 have been identified to be followed by zooplankton in response to the eddy OMZ: i) shallow
39 OMZ avoidance and compression at the surface (e.g. most calanoid copepods, euphausiids),
40 ii) migration to the shallow OMZ core during daytime, but paying O_2 debt at the surface at
41 nighttime (e.g. siphonophores, *Oncaea* spp., eucalanoid copepods), iii) residing in the shallow
42 OMZ day and night (e.g. ostracods, polychaetes), and iv) DVM through the shallow OMZ
43 from deeper oxygenated depths to the surface and back. For strategy i), ii) and iv),
44 compression of the habitable volume in the surface may increase prey-predator encounter
45 rates, rendering zooplankton and micronekton more vulnerable to predation and potentially
46 making the eddy surface a foraging hotspot for higher trophic levels. With respect to long-
47 term effects of ocean deoxygenation, we expect avoidance of the mesopelagic OMZ to set in
48 if oxygen levels decline below approximately $20 \mu\text{mol O}_2 \text{ kg}^{-1}$. This may result in a positive
49 feedback on the OMZ oxygen consumption rates, since zooplankton and micronekton
50 respiration within the OMZ as well as active flux of dissolved and particulate organic matter
51 into the OMZ will decline.

52

53 **1 Introduction**

54 The habitat of pelagic marine organisms is vertically structured by several biotic and abiotic
55 factors, such as light, prey density, temperature, oxygen concentration and others. In the
56 eastern tropical North Atlantic (ETNA), a permanent oxygen minimum zone (OMZ) exists in
57 the mesopelagial. The core of this OMZ is centered at approximately 450 m, with the upper
58 and lower oxyclines at approximately 300 and 600 m depth (Karstensen et al., 2008). Oxygen
59 concentrations in this deep OMZ hardly fall below $40 \mu\text{mol O}_2 \text{ kg}^{-1}$ (Karstensen et al., 2008),
60 but are sufficiently low to exclude highly active top predators such as billfishes from the

61 OMZ (Prince et al., 2010, Stramma et al. 2012). In the eastern tropical South Atlantic, with its
62 more pronounced midwater OMZ, this layer may act as an effective barrier for some species
63 (e.g. Auel and Verheye, 2007; Teuber et al., 2013), but seems to be diurnally crossed by
64 others (Postel et al., 2007). Many zooplankton and nekton taxa perform diurnal vertical
65 migrations (DVMs), usually spending the daylight hours in the mesopelagic OMZ and
66 migrating into the productive surface layer at night. These taxa include for example
67 euphausiids (Tremblay et al., 2011), sergestid and penaeid shrimp (Andersen et al., 1997),
68 myctophid fishes (Kinzer and Schulz, 1985) as well as several large calanoid copepods (e.g.
69 *Pleuromamma* species, Teuber et al., 2013). As DVM is a survival mechanism to evade
70 predation, hindrance thereof could lead to substantial changes in ecosystem functioning. The
71 ETNA OMZ has been observed to intensify (i.e. decrease in core O₂ concentrations) and
72 vertically expand over the past decades and is predicted to further deoxygenate and expand
73 laterally (Stramma et al., 2008; Stramma et al., 2009) under future expectations of
74 anthropogenic global warming (Cocco et al., 2013).

75 Submesoscale and mesoscale eddies (which in the tropics/subtropics comprise diameters on
76 the order of 10¹ and 10² km, respectively) often represent hotspots (or “oases”) of biological
77 productivity in the otherwise oligotrophic open ocean (e.g. Menkes et al., 2002; McGillicuddy
78 et al., 2007; Godø et al., 2012), translating even up to top predators (Tew Kai and Marsac,
79 2010). Their basin-wide relevance for biogeochemical cycles is increasingly recognized (e.g.
80 Stramma et al., 2013). Numerous eddies spin off the productive Mauritanian and Senegalese
81 coast (between Cap Blanc and Cap Vert) throughout the year, with most anticyclones being
82 generated in summer/autumn and most cyclones in winter/spring (Schütte et al., 2015a). Both
83 eddy types propagate westward at about 4 to 5 km day⁻¹, passing the Cape Verde archipelago
84 north or south. They can be tracked by satellite altimetry for up to nine months (Schütte et al.
85 2016; Karstensen et al., 2015). While “normal” anticyclones are usually relatively warm and
86 unproductive (e.g. Palacios et al., 2006), both cyclonic and anticyclonic mode water eddies
87 (ACMEs) are characterized by a negative sea surface temperature (SST) and positive surface
88 chlorophyll-*a* (chl-*a*) anomaly (Goldthwait and Steinberg; 2008; McGillicuddy et al., 2007).
89 In particular, ACMEs were observed to exceed cyclones in terms of upwelled nutrients and
90 productivity in the subtropical Atlantic (McGillicuddy et al., 2007).

91 The recent discovery of mesoscale eddies (cyclones and ACMEs) with extremely low oxygen
92 concentrations just below the mixed layer (Karstensen et al., 2015) has changed our view of

93 current oxygen conditions in the ETNA. In that study, it had been observed that oxygen
94 values $<2 \mu\text{mol O}_2 \text{ kg}^{-1}$ can be found in the shallow oxygen minimum. The authors concluded
95 that the low oxygen concentrations were the result of isolation of the eddy core against
96 surrounding water (a result of the rotation of the eddy) paired with enhanced respiration (a
97 result of the high productivity and subsequent export and degradation of particulate organic
98 matter, Fischer et al., 2015), and introduced the term “dead-zone eddy” (Karstensen et al.
99 2015). The so far lowest oxygen concentrations in such an eddy ($<2 \mu\text{mol O}_2 \text{ kg}^{-1}$ at about
100 40 m depth) were observed in February 2010 at the Cape Verde Ocean Observatory (CVOO)
101 mooring. During the eddy passage across the mooring, an almost complete lack of acoustic
102 scatterers at depth below the oxygenated mixed layer was observed. The acoustic backscatter
103 signal received by the 300 kHz ADCP is largely created by organisms $> 5 \text{ mm}$ (thus missing a
104 substantial part of the mesozooplankton) and does not enable the discrimination of different
105 zooplankton groups.

106 Here, we characterize the ecology of zooplankton in response to the shallow OMZ within an
107 ACME that was identified, tracked and sampled in spring 2014. We used acoustic (shipboard
108 ADCP) and optical (Underwater Vision Profiler) profiling methods as well as vertically
109 stratified plankton net hauls to resolve the vertical and horizontal distribution of zooplankton.
110 Moreover, we used acoustic and oxygen time series data from the CVOO mooring of one
111 extreme low oxygen eddy observed in February 2010 (Karstensen et al. 2015, Fischer et al.
112 2015) to derive a more general picture about the zooplankton sensitivity to low oxygen
113 concentrations.

114

115 **2 Materials and Methods**

116 In order to characterize the ecology, biogeochemistry and physical processes associated with
117 low oxygen eddies in the tropical North Atlantic, a dedicated field experiment (“eddy hunt”)
118 north of the Cape Verde Archipelago was designed. In summer 2013, the identification and
119 tracking of candidate eddies was started by combining remotely sensed data and Argo float
120 profile data. In spring 2014, a candidate low oxygen eddy was identified and on-site sampling
121 with gliders and research vessels began, covering genomics, physics, and biogeochemistry
122 (see also Löscher et al. 2015, Schütte et al. 2016, Fiedler et al. 2016, , Karstensen et al. 2016;
123 this issue). Ship-based sampling (“site survey”) presented here was carried out on March 18th

124 and 19th, 2014 during the RV *Meteor* cruise M105. Two ADCP sections perpendicular to each
125 other, a CTD/UVP5 cast section, and five multinet hauls were conducted. To better
126 characterize the average distribution of zooplankton during “normal” conditions in the
127 investigation area (as compared to conditions within the eddy), we combined the single time
128 point observation at the CVOO time series station with previously collected data at the same
129 station. For the multinet data, we used three additional day/night casts (RV *Maria S. Merian*
130 cruise MSM22: Oct 25, 2012 and Nov 20, 2012; RV *Meteor* cruise M97: May 26, 2013). For
131 the UVP data, we used seven nighttime profiles (because the four eddy core stations were
132 obtained during nighttime only) from cruises M105, MSM22, M97 and M106 (April 19/20,
133 2014). All data are publically available in the PANGAEA database
134 (<http://doi.pangaea.de/10.1594/PANGAEA.858323>).

135 In order to evaluate in greater detail the critical oxygen concentrations that lead to avoidance
136 behaviour we used the mean volume backscatter (S_v) and oxygen time series data from the
137 CVOO mooring. Here, we focus on the spring 2010 period that covered the transit of an
138 extreme low oxygen eddy, with oxygen content $<2\mu\text{mol kg}^{-1}$ (Karstensen et al., 2015).

139 **2.1 ADCP**

140 Underway current measurements were performed during cruise M105 using two vessel
141 mounted Acoustic Doppler Current Profilers (vmADCP), a 75kHz RDI Ocean Surveyor
142 (OS75) and a 38kHz RDI Ocean Surveyor (OS38). Standard techniques (see Fischer et al.,
143 2003) were used for data post-processing. Depending on the region and sea state, the ranges
144 covered by the instruments are around 550 m for the OS75 and around 1000 m for the OS38.
145 To locate the eddy center from the observed velocities, two sections were conducted (Fig. 1).
146 The first was a southeast-to-northwest section through the estimated (by remote sensing) eddy
147 center. The second section was a perpendicular, northeast-to-southwest section through the
148 location of lowest cross-sectional current velocity of the first section. The lowest cross-
149 sectional velocity of the second section defines the eddy center.

150 The ADCP installed at the CVOO mooring site in 109 m water depth was an upward looking
151 300kHz Teledyne RDI workhorse instrument, recording data every 1.5 hours. It has a 4 beam
152 design in Janus configuration with 20° opening. Based on accompanying hydrographic and
153 pressure data, each 4 m depth cell was allocated a discrete pressure/depth information as well
154 as a sound speed profile (harmonic mean). S_v from the four ADCP beams was averaged and

155 matched to the oxygen data (i.e., backscatter values in the depth cell where the oxygen sensor
156 was located were used, which varied around approximately 50 m dependent on the current
157 strength). Only data from January 1, 2010 to March 14, 2010 were used for the analysis to
158 avoid the influence of seasonal changes in scatterer abundance. Data collected from 11:00 to
159 18:00 UTC and from 22:00 to 07:00 UTC were considered daytime and nighttime data,
160 respectively. Apparent sunrise and sunset in the period of January to March are around 08:00
161 and 19:30 UTC, respectively.

162 For vessel-mounted as well as moored ADCP, the mean volume backscatter S_v (MacLennan
163 et al, 2002) was estimated for each beam and each depth cell by a recalculation of a simplified
164 sonar equation (Deimes 1999). From the vessel-mounted ADCPs, only the OS75 was used to
165 assess backscatter distribution. Because we were not attempting to estimate biomass, no
166 further calibration was applied and S_v are values are relative.

167 **2.2 CTD and UVP5**

168 Oxygen concentration was measured using a SBE CTD with two SBE 43 oxygen sensors. The
169 oxygen sensors were calibrated against 641 discrete oxygen samples measured by Winkler
170 titration during cruise M105. Inside the CTD-rosette, a UVP5 was mounted. This imaging
171 tool allows *in situ* quantification of particles $>60 \mu\text{m}$ and plankton $>500 \mu\text{m}$ with high vertical
172 resolution (Picheral et al., 2010). Thumbnails of all objects $> 500 \mu\text{m}$ were extracted using the
173 ImageJ-based ZooProcess macro set (Gorsky et al., 2010) and sorted automatically into 41
174 categories using Plankton Identifier (Gasparini, 2007). Experts validated the automated image
175 sorting. The observed volume of each image was 0.93 L and approximately ten images were
176 recorded per meter depth. The mean total sampling volume for the upper 600 m of the water
177 column was $6.34 (\pm 0.99) \text{ m}^3$. Volume-specific abundance was calculated in 5 m depth bins.

178 **2.3 Multinet**

179 Zooplankton samples were collected with a Hydrobios multinet Midi (0.25 m^2 mouth
180 opening, 5 nets, 200 μm mesh, equipped with flowmeters) hauled vertically from the
181 maximum depth to the surface at 1 m s^{-1} .

182 A full “day/night” multinet station was conducted well outside of the eddy at 17.3474° N and
183 24.1498° W at the CVOO site, where a set of physical and biogeochemical variables are
184 measured on a monthly basis. For this reason, CVOO standard depths were used in this

185 multinet haul (800-600-300-200-100-0 m) as it also served the time series observations. As
186 the NW-ward eddy transect was conducted during daytime, the “eddy core day” multinet haul
187 was collected on this transect (12:40 UTC) and the “eddy core night” haul was collected at
188 02:10 UTC during the second transect (for classification of stations, see hydrography results
189 section), at the location of the CTD profile with the lowest O₂ concentration. Thus, the “eddy
190 core day” haul is approximately 14 km away from the eddy center (Fig.1). Depth intervals
191 (600-300-200-120-85-0 m) were chosen according to the O₂ profile. When leaving the eddy, a
192 second “day” haul was collected at the margin of the eddy, approximately 26 km from the
193 eddy center, using the depth intervals from the eddy core station. Zooplankton samples were
194 fixed in 100 mL Kautex® jars in 4% borax-buffered formaldehyde in seawater solution.

195 Zooplankton samples were analysed using a modification of the ZooScan Method (Gorsky et
196 al., 2010), employing an off-the-shelf flatbed scanner (Epson Perfection V750 Pro) and a scan
197 chamber constructed of a 21 cm x 29.7 cm (DIN-A4) size glass plate with a plastic frame.
198 Scans were 8bit grayscale, 2400 dpi images (Tagged image file format; *.tif). The scan area
199 was partitioned into two halves (i.e., two images per scanned frame) to reduce the size of the
200 individual images and facilitate the processing by ZooProcess/ImageJ. Samples were size-
201 fractionated by sieving into three fractions (<500 µm, 500-1000 µm, >1000 µm) and split
202 using a Motoda plankton splitter if necessary. The >1000 µm fraction was scanned
203 completely, whereas fractions comprising not more than approximately 1000 objects were
204 scanned for the two other fractions. “Vignettes” and image characteristics of all objects were
205 extracted with ZooProcess (Gorsky et al., 2010) and sorted into 39 categories using Plankton
206 Identifier (Gasparini, 2007). Automated image sorting was then manually validated by
207 experts.

208

209 **3 Results**

210 **3.1 Hydrography**

211 The site survey with RV Meteor succeeded in sampling the eddy core with CTD and UVP
212 casts. The lowest measured O₂ concentration was 3.75 µmol O₂ kg⁻¹ at 106 m depth. Based
213 upon the current velocity, the eddy was approximately 110 km in diameter (Fig. 1), but
214 oxygen concentrations below 20 and 5 µmol O₂ kg⁻¹ were only found within approximately
215 18 and 8 km from the center, respectively. For the purpose of this study, the four stations

216 within 20 km to the eddy core (with minimum O₂ concentrations well below 20 μmol O₂ kg⁻¹)
217 ¹) were considered “eddy core”, while the four stations within 20 to 35 km from the eddy core
218 were considered “eddy margin” (with minimum O₂ concentrations between 21 and 53 μmol
219 O₂ kg⁻¹) and the CVOO station (M105 data complemented with data from previous cruises,
220 n=7 profiles, see methods) was considered to represent ambient conditions outside of the
221 eddy. Here, a shallow OMZ was not present. The midwater OMZ (centered around
222 approximately 450 m depth) featured mean minimum oxygen concentrations of 70 μmol O₂
223 kg⁻¹.

224

225 **3.2 Vertical distribution and DVM – acoustic observations**

226 During the M105 ADCP survey, several features were apparent in the vertical distribution and
227 migration of scatterers outside of the eddy (Fig. 2). First, a deep scattering layer was detected
228 centered between below 350 and 400 m depth. From this layer, part of the population started
229 its ascent to the surface layer at about 18:00 UTC. The center of the nighttime distribution
230 outside the eddy ranged from approximately 30 to 130 m depth. During the day, lowest S_v
231 was recorded between 100 and 300 m depth, with a residual non-migrating population in the
232 upper 100 m. The ascendant and descendent migration took place from approximately 18:00
233 to 20:00 UTC (16:15 to 18:15 solar time) and 07:00 to 09:00 UTC (05:15 to 07:17 solar
234 time), respectively.

235 A very different nighttime distribution was observed when traversing the eddy. The scatterers
236 in the surface layer were located further up in the water column than outside the eddy and
237 their lower distribution margin coincided with the upper oxycline (approximately 85 m in the
238 eddy center). In the core of the shallow OMZ, below approximately 20 μmol O₂ kg⁻¹, an
239 absolute minimum S_v was observed.

240 The intersection of the two transects (see red crosses in Fig. 2) was visited shortly after 12:00
241 and 00:00 UTC, representing full day/night conditions, respectively. Here, the difference
242 between S_v in the surface at day and night suggests substantial vertical migration into/out of
243 the surface layer, crossing the OMZ (Fig 2.b). Also, the distribution of the surface daytime
244 resident population (with S_v values of approximately 75dB) is bimodal, peaking again at
245 approximately 90 m. This is well within the shallow OMZ (note that there are no O₂ isolines

246 shown in the daytime transect in Fig. 2b since there were no CTD casts performed on the first
247 transect).

248 Reanalysis of acoustic backscatter and oxygen time series data from the CVOO mooring
249 before and during the transit of an ACME in 2010 (Karstensen et al. 2015) shows that the
250 daytime S_v at the depth level of the oxygen sensor (around 50 m, depending on wire angle) is
251 reduced below approximately $20 \mu\text{mol O}_2 \text{ kg}^{-1}$ (Fig. 3a, power function; $r^2=0.69$). For the
252 nighttime data (Fig. 3b), the relationship between S_v and oxygen concentration is best
253 described by a linear function ($r^2=0.94$). S_v in the subsurface increases around approximately
254 07:00 and 19:00 UTC (supplementary figure S1). These dusk and dawn traces suggest that
255 DVM species migrate through the OMZ even when the daily mean oxygen concentration is
256 between 5 and $20 \mu\text{mol kg}^{-1}$.

257 **3.3 Optical Profiling**

258 The UVP5 transect across the eddy revealed a pronounced increase of aggregates in the eddy
259 core (Fig. 4a). This pattern was still evident at the maximum profile depth (600 m, below the
260 midwater OMZ). At the same time, surface abundance of copepods (Fig. 4b) and, to a lesser
261 degree, collodaria (Fig. 4c) is higher than in surrounding waters. Copepods were observed in
262 substantial abundance within the OMZ, while collodaria appeared to avoid it. On the other
263 hand, gelatinous zooplankton (comprising medusae, ctenophores, and siphonophores, Fig. 3d)
264 were observed in the inner OMZ core. Not a single observation of shrimp-like micronekton
265 (euphausiids and decapods, Fig. 4e) was made at oxygen concentrations lower than $28 \mu\text{mol}$
266 $\text{O}_2 \text{ kg}^{-1}$. Integrated abundance (upper 600 m, Fig. 5) of large aggregates was significantly
267 higher in the “core” stations compared to the “outside” (one-way ANOVA, Tukey’s HSD
268 $p<0.001$) and “margin” ($p<0.05$) stations. The integrated abundance of gelatinous plankton
269 was significantly higher in the “core” stations than in the “outside” stations ($p<0.05$). For the
270 other groups, differences in integrated abundance were not significant.

271 **3.4 Multinet**

272 The multinet data provides a higher taxonomic resolution, but lower spatial (horizontal and
273 vertical) resolution than the optical profiles (UVP). In Fig. 6, the abundance and vertical
274 distribution of eight conspicuous taxa are depicted, ordered by their apparent sensitivity to
275 hypoxia. While euphausiids (Fig. 6a), calanoid copepods (Fig. 6b) and foraminifera (Fig. 6c)

276 are abundant in the surface layer (exceeding the mean abundance at CVOO), they appear to
277 avoid the shallow OMZ. Siphonophores (Fig. 6d), the poecilostomatoid *Oncaea* spp. (Fig. 6e)
278 and eucalanoid copepods (Fig. 6f) are all very abundant in the eddy's surface layer during the
279 night (with the latter also being observed in the shallow OMZ during nighttime) and appear to
280 take refuge within the shallow OMZ during daylight hours. Two groups that appeared to
281 favour the shallow OMZ even during nighttime hours were polychaetes (Fig. 6g) and
282 ostracods (Fig. 6h), but also the harpacticoid copepod *Macrosetella gracilis* (Table S1). Taxa
283 that were more abundant in the surface layer of the eddy core compared to the mean outside
284 eddy situation, included eucalanoid and other calanid copepods, *Oithona* spp., *Macrosetella*
285 *gracilis*, *Oncaea* spp., ostracods, decapods, siphonophores, chaetognaths, molluscs (mainly
286 pteropods), polychaetes and foraminifera (Table S1). In contrast, taxa that were less abundant
287 in the surface layer in the eddy were amphipods, salps and appendicularia. Although not
288 sampled quantitatively by this type of net, this also seemed to be the case for fishes. In
289 particular, no single individual was caught in the upper 200 m of the eddy core night station.
290 Total area-integrated abundance of all zooplankton organisms in the upper 600 m was
291 151,000(\pm 34,000) m⁻² in the eddy core and 101,000(\pm 15,000) at the "outside" station (Table
292 S2).

293

294 **4 Discussion**

295 Already during the remote survey, it became apparent that the tracked mesoscale eddy was a
296 hotspot of primary productivity. Lowered sea surface temperature and elevated surface chl-*a*
297 values (satellite imagery; Schütte et al., 2015a) as well as increased nitrate levels in the eddy
298 interior (autonomous gliders; Karstensen et al., 2016, Fiedler et al., 2016) indicate active
299 upwelling and translate into substantially increased productivity (Löscher et al., 2015).
300 During westward propagation, the hydrographic character was found to be remarkably
301 constant (Karstensen et al., 2016; Schütte et al., 2016), while the genomic characterization
302 (Löscher et al., 2015) as well as the particle composition (Fischer et al., 2015) indicate that
303 the eddy has created a unique ecosystem that has not much in common with the coastal one it
304 originated from. The present study is the first to observe the impact of such eddies on pelagic
305 metazoans. Since process understanding and zooplankton production estimates are still
306 lacking, we cannot conclude whether the system is ultimately bottom-up or top-down

307 controlled and whether the seemingly high zooplankton productivity may be due to lacking
308 higher trophic levels.

309 We deliberately chose not to attempt a direct comparison of methods (e.g. by trying to derive
310 biomass from ADCP backscatter), but rather use the three methods complementary to each
311 other: The acoustic survey reveals the horizontal and vertical fine-scale spatial distribution of
312 scatterers (macrozooplankton and micronekton). It suggests a complete avoidance of the
313 OMZ by these groups, whose identity remains somewhat unclear (see also Karstensen et al.,
314 2015). The UVP has an excellent vertical and an intermediate horizontal (several profiles
315 along transect) resolution, with restricted information regarding the identity of the organisms
316 (limited by image resolution and sampling volume to more abundant mesozooplankton). The
317 multinet has low vertical and horizontal resolution, and low catch efficiency for fast-
318 swimming organisms. Its main asset is that it allows a detailed investigation of zooplankton
319 and some micronekton organisms. Since the samples are still intact after scanning,
320 taxonomists interested in one of the groups presented here would even be able to proceed with
321 more detailed work.

322 Using the shipboard and moored ADCP to investigate acoustic backscatter (rather than a
323 calibrated scientific echosounder) resulted from the necessity to gather ADCP-derived current
324 velocity data for eddy identification and localization of the core (see Fig. 1). It has to be noted
325 that the backscatter signals from the 75 kHz shipboard ADCP and the 300 KHz moored
326 ADCP are strictly not comparable as for organisms that are small compared to the acoustic
327 wavelengths, the backscatter strength increases rapidly with increasing frequency (Stanton et
328 al., 1994). Also, smaller organisms contribute more to the 300 kHz signal than to the 75 kHz.
329 Still, both instruments suggest that OMZ avoidance sets in at O_2 concentrations lower than
330 approximately $20 \mu\text{mol } O^2 \text{ kg}^{-1}$.

331 The marked decrease in ADCP S_v in the shallow OMZ is only partly confirmed by the other
332 two techniques. The animals that contribute most to the ADCP backscatter at a frequency of
333 75 kHz are targets in the cm-size range (75kHz correspond to a wavelength of 20 mm), i.e.
334 larger zooplankton and micronekton such as euphausiids, amphipods, small fish, pteropods,
335 siphonophores and large copepods (Ressler, 2002). Thus, the community of organisms
336 contributing most to the backscatter is not quantitatively (i.e., providing accurate abundance
337 estimates) sampled by the multinet and the UVP5. Both mostly target organisms < 10 mm in
338 size and the sampling volume is small, in particular with the UVP5. Still, spatial observation

339 patterns of these organisms derived from the multinet and UVP5 may help to provide
340 explanations for the patterns observed in the ADCP, even though abundance estimates are to
341 be taken with caution. For example, euphausiids contribute substantially to the backscatter at
342 75kHz in this region (as observed through horizontal MOCNESS tows during dusk and dawn
343 resolving ADCP migration traces, Buchholz, Kiko, Hauss, Fischer unpubl.). Thus, the relative
344 decrease of observed euphausiids in the OMZ (and in the eddy in general) in both multinet
345 samples and UVP profiles suggests that they may be partly responsible for the lack of
346 backscatter in the OMZ.

347 High-resolution profiles obtained by the UVP5 indicated OMZ avoidance by euphausiids and
348 collodaria, while copepods (albeit at lower concentrations than in the surface layer) were
349 observed in the OMZ core. Gelatinous zooplankton was even more abundant in the shallow
350 OMZ than in surface waters. The multinet data (providing higher taxonomic resolution and
351 larger sampling volume, but lower vertical resolution) suggest that there are four strategies
352 followed by zooplankton in the eddy, which will be discussed below.

353 *i) shallow OMZ avoidance and compression at the surface*

354 We ascribe this behaviour to euphausiids and most calanoid copepods as well as collodaria
355 and foraminifera (from the supergroup rhizaria). While the total abundance of krill is probably
356 underestimated by the comparatively slow and small plankton net, their vertical distribution in
357 relation to the OMZ and the marked total decrease within the eddy compared to “outside”
358 stations suggests that they are susceptible to OMZ conditions and may suffer from increased
359 predation in the surface layer. This is in line with physiological observations, where a critical
360 partial pressure of 2.4 and 6.2 kPa (29.6 and 64.2 $\mu\text{mol O}_2 \text{ kg}^{-1}$) was determined at subsurface
361 (13°C) and near-surface temperature (23°C), respectively, in *Euphausia gibboides* in the
362 ETNA (Kiko et al., 2015). Calanoid copepods represent the largest group in terms of
363 abundance and biomass and comprise approximately one hundred species in Cape Verdean
364 waters (Séguin, 2010) with a wide range of physiological and behavioural adaptations.
365 Species most tolerant to low-oxygen conditions are vertically migrating species such as
366 *Pleuromamma* spp., while epipelagic species such as *Undinula vulgaris* are less tolerant
367 (Teuber et al., 2013; Kiko et al., 2015). From the rhizaria supergroup, the fine-scale
368 distribution pattern of solitary collodaria (a group that is abundant in surface waters of the
369 oligotrophic open ocean, see Biard et al., 2015 and references therein) suggests OMZ
370 sensitivity, but direct evidence from the literature is lacking. The foraminifera, which are

371 mostly too small to be quantified well with the UVP5, but in contrast to other rhizaria are well
372 preserved in buffered formaldehyde in seawater solution, were highly abundant in the surface
373 of the eddy core. Here, the distribution shift likely also includes a community shift, since a
374 marked dominance change from surface-dwelling to subsurface-dwelling species was found
375 in sediment trap data during the transit of the 2010 ACME (Fischer et al., 2015). In that
376 ACME, also an export flux peak by foraminifera was observed.

377 *ii) migration to the shallow OMZ core during daytime*

378 This strategy seems to be followed by siphonophores, *Oncaea* spp., and eucalanoid copepods.
379 Although it seems unlikely that siphonophores in this survey were contributing substantially
380 to the ADCP backscatter, as those retrieved by the multinet were almost exclusively
381 calycothorans (see Fig. 6d for a type specimen) which do not have a pneumatophore and,
382 therefore, lack gas bubbles that are highly resonant in other siphonophore groups (e.g.
383 Ressler, 2002). They may, however, contribute to the weak backscatter signal in the shallow
384 OMZ during daytime (Fig. 2b and 6d). *Oncaea* spp. are particle-feeding copepods that are
385 directly associated with marine snow (Dagg et al., 1980). They were observed in quite
386 extreme OMZs in other oceanic regions (e.g. Böttger-Schnack, 1996; Saltzman & Wishner,
387 1997), however, our results suggest that at least in the tropical Atlantic biome they cannot
388 permanently endure hypoxia but have to pay their oxygen debt during nighttime. The majority
389 of adult eucalanoid copepods were *Rhincalanus nasutus*, a species that is frequently found in
390 the midwater OMZ of the ETNA. In the eastern tropical Pacific, however, *R. nasutus* was
391 reported to be excluded from the extreme midwater OMZ (500-1000 m depth, below
392 approximately 22 $\mu\text{mol O}_2 \text{ kg}^{-1}$), unlike the key OMZ-adapted eucalanoid species of that
393 region (e.g. *Eucalanus inermis*), which are able to permanently inhabit the OMZ (Saltzman &
394 Wishner, 1997). In our study, *R. nasutus* were found also in the shallow (extreme) OMZ of
395 the eddy (well below 20 $\mu\text{mol O}_2 \text{ kg}^{-1}$), indicating that this copepod species may be also able
396 to cope with further deoxygenation of the midwater OMZ in the Atlantic. Both *Oncaea* and
397 *Rhincalanus* are unlikely to be seen in the S_v signal at 75 kHz.

398 *iii) residing in the shallow OMZ day and night*

399 Contrary to most crustaceans, collodaria and euphausiids, a remarkable ability to endure OMZ
400 conditions for prolonged periods of time seems to be present in ostracods, polychaetes,
401 *Macrosetella gracilis* and gelatinous plankton. “Jellies” are a group of organisms of which
402 several taxa, such as siphonophores, salps, hydromedusae and ctenophores, have been

403 reported to tolerate hypoxic conditions much better than most crustacean zooplankton (Mills
404 2001; Thuesen et al. 2005). In addition to reduced metabolic activity (e.g. Rutherford and
405 Thuesen, 2005), using the mesoglea gel matrix as an oxygen reservoir was shown to be a
406 strategy in scyphomedusae to temporarily survive anoxia (Thuesen et al. 2005). It has also
407 been suggested that “jellyfish” (i.e., pelagic cnidarians and ctenophores) outcompete other
408 planktonic groups in coastal systems under eutrophication-induced hypoxia (Mills 2001). The
409 UVP5 nighttime section suggests that many gelatinous organisms reside within the shallow
410 OMZ even during nighttime. This is only partly confirmed by the multinet data; however,
411 ctenophores and medusae are often destroyed during sampling and not well preserved in
412 formaldehyde. For ostracods, it is known that several limnic (Teixeira et al. 2014) and marine
413 (Corbari et al. 2004) benthic species tolerate hypoxia for prolonged periods of time (and
414 preferentially select hypoxic habitats over oxygenated ones), which lead to the use of their
415 abundance in sediment cores as a proxy for past ocean oxygenation (Lethiers and Whatley,
416 1994). In pelagic marine ostracods, however, there is little evidence for particular
417 preadaptation to OMZ conditions. To the best of our knowledge, no physiological studies
418 exist that describe the metabolic response of pelagic ostracods to hypoxia. Recently, it was
419 found that the oxygen transport protein hemocyanin occurs in several groups within the class
420 ostracoda, including planktonic species (Marxen et al. 2014). In the Arabian Sea, highest
421 ostracod abundances were found in the oxygenated surface layer, but consistent occurrence in
422 the extreme OMZ ($<5 \mu\text{mol O}_2 \text{ kg}^{-1}$) was reported (Böttger-Schnack, 1996). In the eastern
423 tropical Pacific, most species were reported to avoid the OMZ, with the notable exception of
424 *Conchoecetta giesbrechti*, which is classified as an OMZ-adapted species (Castillo et al.,
425 2007). For pelagic polychaetes, Thuesen and Childress (1993) even state that they may have
426 the highest metabolic rates (and, thus, oxygen demand) in the meso- and bathypelagic zones
427 of the oceans, with the exception of the aberrant species *Poebobius meseres*.

428 *iv) migration through the shallow OMZ core to better-oxygenated depths*

429 To rigorously assess DVM reduction by the underlying OMZ, acoustic 24h-observations
430 would be necessary to directly observe the migration pattern. Unfortunately, the dawn and
431 dusk migration observations took place at the NE- and SW-margin of the eddy, respectively,
432 just outside the $30 \mu\text{mol O}_2 \text{ kg}^{-1}$ boundary (Fig. 2). Nevertheless, it appears from the
433 day/night difference in the shipboard ADCP S_v (at the intersection of the two transects) as
434 well as from the moored ADCP data (Fig S1) that at least part of the migrating population

435 “holds its breath” and crosses the OMZ during ascent/descent. In this respect, the thin shallow
436 OMZ seems to be different from the several hundred meters thick mesopelagic OMZ, which
437 at low core oxygen concentrations can serve as a quite effective migration barrier (Auel and
438 Verheye, 2007; Teuber et al., 2013).

439 The enhanced surface primary productivity of the eddy also resulted in an approximately 5-
440 fold increase of large particles, well visible down to 600 m depth. This indicates a massive
441 export flux by sinking marine snow (see also Fischer et al. 2015 for sediment trap data of the
442 2010 ACME), which is thus made available to higher trophic levels at greater depths. As an
443 example, phaeodaria (in supergroup rhizaria) are one of the few exclusively mesopelagic
444 groups (only found deeper than approximately 200 m in UVP profiles). Their integrated
445 abundance seemed to be positively affected by the eddy conditions, which may indicate
446 favourable feeding/growth conditions at depth.

447 In summary, mesozooplankton biomass was generally enhanced in the euphotic zone of the
448 ACME, suggesting that it may represent an “oasis in the desert” *sensu* Godø et al. (2012),
449 although the differences to “outside” conditions were not quite as large as those reported by
450 Goldthwait and Steinberg (2008). On the other hand, subsurface hypoxia appears to be
451 detrimental to some surface-dwelling as well as vertically migrating zooplankton taxa. We
452 lack quantitative estimates of higher trophic levels (the multinet is too small and slow to
453 efficiently sample fast-swimming nekton organisms), but it seems that the small migratory
454 mesopelagic fishes which were usually caught (albeit in low numbers) outside the eddy were
455 less abundant in the eddy core’s surface. To draw robust conclusions on the identity and
456 whereabouts of acoustic scatterers, the additional use of several types of stratified nets is
457 necessary (e.g. 10 m² MOCNESS in addition to a multinet or 1 m² MOCNESS) but was
458 logistically impossible during the opportunistic sampling on M105. Since gelatinous plankton
459 organisms appear to play a key role in these oceanic OMZs and are notoriously undersampled
460 by nets and/or destroyed by fixatives, it even seems worthwhile to employ a dedicated camera
461 system (with larger sampling volume than the UVP5) for such a survey. It also remains an
462 open question whether the rich zooplankton prey field is exploited by epipelagic fishes and
463 their predators (see e.g. Tew Kai and Marsac, 2010 for examples of tuna and seabird
464 interaction with cyclonic eddies). By providing isolated bodies of water with distinct (and
465 sometimes, like in our case, extreme) environmental conditions for many months, mesoscale
466 eddies are important vectors of species dispersal and invasion (Wiebe and Flierl, 1983) and

467 subject the population fragments they contain to their own mutations, selection forces, and
468 genetic drift effects. Thus, they are not only hypothesized to play a central role in speciation
469 of planktonic species (Bracco et al. 2000, Clayton et al. 2013), but may resemble a key
470 mechanism to equip oceanic metapopulations with the range of physiological and behavioural
471 adaptations deemed necessary to survive under global change.

472

473 **5 Conclusions**

474 Acoustic observations (shipboard ADCP) confirm previous observations (moored ADCP) of a
475 sharp decrease in backscatter at O₂ concentrations below approximately 20 μmol O₂ kg⁻¹.
476 Euphausiids (which are known to contribute substantially to the ADCP backscatter) were not
477 observed within the OMZ stratum of the eddy, and their integrated abundance was markedly
478 reduced. Still, multinet and UVP5 data indicate that several zooplankton groups are
479 surprisingly insensitive to these extreme OMZ conditions, and many taxa that avoid the OMZ
480 even reach higher abundance in the productive surface environment of the eddy. However, it
481 remains an open question if and how higher trophic levels (such as small pelagic forage fish
482 and their predators) may benefit from the dense prey field. While the term “open ocean dead
483 zone” may be an exaggeration, low-oxygen eddies in the ETNA in the light of future
484 deoxygenation might serve as a crystal ball (or, more appropriately, a “scrying pool”) to
485 estimate the differential response of different plankton functional groups of the open ocean to
486 global change.

487

488 **Acknowledgements**

489 We are particularly grateful to the chief scientists of M105, Martin Visbeck and Toste
490 Tanhua, for shaving two days off their tight cruise schedule to make this survey happen. This
491 work is a contribution of the Future Ocean Excellence Cluster project CP1341
492 “Biogeochemistry and Ecology of Oxygen Depleted Eddies in the Eastern Tropical Atlantic”
493 and of the SFB 754 "Climate - Biogeochemistry Interactions in the Tropical Ocean"
494 (www.sfb754.de) which is supported by the German Science Foundation (DFG).

495

496 **References**

497 Andersen, V., Sardou, J., and Gasser, B.: Macroplankton and micronekton in the northeast
498 tropical Atlantic: abundance, community composition and vertical distribution in relation to
499 different trophic environments, *Deep Sea Research Part I: Oceanographic Research Papers*,
500 44, 193-222, 1997.

501 Auel, H. and Verheye, H. M.: Hypoxia tolerance in the copepod *Calanoides carinatus* and the
502 effect of an intermediate oxygen minimum layer on copepod vertical distribution in the
503 northern Benguela Current upwelling system and the Angola–Benguela Front, *Journal of*
504 *Experimental Marine Biology and Ecology*, 352, 234-243, 2007.

505 Biard, T., Pillet, L., Decelle, J., Poirier, C., Suzuki, N., and Not, F.: Towards an Integrative
506 Morpho-molecular Classification of the Collodaria (Polycystinea, Radiolaria), *Protist*,
507 doi:10.1016/j.protis.2015.05.002, 2015.

508 Böttger-Schnack, R.: Vertical structure of small metazoan plankton, especially noncalanoid
509 copepods. I. Deep Arabian Sea, *Journal of Plankton Research*, 18, 1073-1101, 1996.

510 Bracco, A., Provenzale, A., and Scheuring, I.: Mesoscale vortices and the paradox of the
511 plankton, *Proceedings of the Royal Society of London B: Biological Sciences*, 267, 1795-
512 1800, 2000.

513 Castillo, R., Antezana, T., and Ayon, P.: The influence of El Nino 1997–98 on pelagic
514 ostracods in the Humboldt Current Ecosystem off Peru, *Hydrobiologia*, 585, 29-41, 2007.

515 Clayton, S., Dutkiewicz, S., Jahn, O., and Follows, M. J.: Dispersal, eddies, and the diversity
516 of marine phytoplankton, *Limnology and Oceanography: Fluids and Environments*, 3, 182-
517 197, 2013.

518 Cocco, V., Joos, F., Steinacker, M., Frölicher, T., Bopp, L., Dunne, J., Gehlen, M., Heinze,
519 C., Orr, J., and Oeschlies, A.: Oxygen and indicators of stress for marine life in multi-model
520 global warming projections, *Biogeosciences*, 10, 1849-1868, 2013.

521 Corbari, L., Carbonel, P., and Massabuau, J.-C.: How a low tissue O₂ strategy could be
522 conserved in early crustaceans: the example of the podocopid ostracods, *Journal of*
523 *experimental biology*, 207, 4415-4425, 2004.

524 Dagg, M., Cowles, T., Whitley, T., Smith, S., Howe, S., and Judkins, D.: Grazing and
525 excretion by zooplankton in the Peru upwelling system during April 1977, *Deep Sea Research*
526 *Part I: Oceanographic Research Papers*, 27, 43-59, 1980.

527 Deimes, K.L., Backscatter Estimation Using Broadband Acoustic Doppler Current Profilers,
528 Proceedings of the IEEE Sixth Working Conference on Current Measurement, San Diego,
529 CA, March 11-13 1999. pp.249-253, DOI: 10.1109/CCM.1999.755249, 1999.

530 Fiedler, B., Grundle, D., Schütte, F., Karstensen, J., Löscher, C. R., Hauss, H., Wagner, H.,
531 Loginova, A., Kiko, R., Silva, P., and Körtzinger, A.: Oxygen Utilization and Downward
532 Carbon Flux in an Oxygen-Depleted Eddy in the Eastern Tropical North Atlantic,
533 Biogeosciences Discuss., 2016, 1-35, 2016.

534 Fischer, J., Brandt, P., Dengler, M., Müller, M., and Symonds, D.: Surveying the upper ocean
535 with the Ocean Surveyor: a new phased array Doppler current profiler, Journal of
536 Atmospheric and Oceanic Technology, 20, 742-751, 2003.

537 Fischer, G., Karstensen, J., Romero, O., Baumann, K-H., Donner, B., Hefter, J., Mollenhauer,
538 G., Iversen, M., Fiedler, B., Monteiro, I. and Körtzinger, A.: Bathypelagic particle flux
539 signatures from a suboxic eddy in the oligotrophic tropical North Atlantic: production,
540 sedimentation and preservation, Biogeosciences Discuss., 12, 18253-18313, 2015..

541 Gasparini, S.: PLANKTON IDENTIFIER: a software for automatic recognition of planktonic
542 organisms. http://www.obs-vlfr.fr/~gaspari/Plankton_Identifier/index.php, last access
543 11/11/2015, 2007.

544 Godø, O. R., Samuelsen, A., Macaulay, G. J., Patel, R., Hjøllø, S. S., Horne, J., Kaartvedt, S.,
545 and Johannessen, J. A.: Mesoscale eddies are oases for higher trophic marine life, PLoS One,
546 7, e30161, doi: 10.1371/journal.pone.0030161, 2012.

547 Goldthwait, S. A. and Steinberg, D. K.: Elevated biomass of mesozooplankton and enhanced
548 fecal pellet flux in cyclonic and mode-water eddies in the Sargasso Sea, Deep Sea Research
549 Part II: Topical Studies in Oceanography, 55, 1360-1377, 2008.

550 Gorsky, G., Ohman, M. D., Picheral, M., Gasparini, S., Stemann, L., Romagnan, J.-B.,
551 Cawood, A., Pesant, S., García-Comas, C., and Prejger, F.: Digital zooplankton image
552 analysis using the ZooScan integrated system, Journal of Plankton Research, 32, 285-303,
553 2010.

554 Karstensen, J., Stramma, L., and Visbeck, M.: Oxygen minimum zones in the eastern tropical
555 Atlantic and Pacific oceans, Progress in Oceanography, 77, 331-350, 2008.

556 Karstensen, J., Fiedler, B., Schütte, F., Brandt, P., Körtzinger, A., Fischer, G., Zantopp, R.,
557 Hahn, J., Visbeck, M., and Wallace, D.: Open ocean dead zones in the tropical North Atlantic
558 Ocean, *Biogeosciences*, 12, 2597-2605, 2016.

559 Karstensen, J., Schütte, F., Pietri, A., Krahnemann, G., Fiedler, B., Grundle, D., Hauss, H.,
560 Körtzinger, A., Löscher, C., and Viera, N.: Anatomy of open ocean dead-zones based on
561 high-resolution multidisciplinary glider data, *Biogeosciences Discuss.*, 2016.

562 Kiko, R., Hauss, H., Buchholz, F., and Melzner, F.: Ammonium excretion and oxygen
563 respiration of tropical copepods and euphausiids exposed to oxygen minimum zone
564 conditions, *Biogeosciences Discuss.*, 12, 17329-17366, 2015.

565 Kinzer, J. and Schulz, K.: Vertical distribution and feeding patterns of midwater fish in the
566 central equatorial Atlantic, *Marine Biology*, 85, 313-322, 1985.

567 Lethiers, F. and Whatley, R.: The use of Ostracoda to reconstruct the oxygen levels of Late
568 Palaeozoic oceans, *Marine Micropaleontology*, 24, 57-69, 1994.

569 Löscher, C. R., Fischer, M. A., Neulinger, S. C., Fiedler, B., Philippi, M., Schütte, F., Singh,
570 A., Hauss, H., Karstensen, J., Körtzinger, A., Künzel, S., and Schmitz, R. A.: Hidden
571 biosphere in an oxygen-deficient Atlantic open-ocean eddy: future implications of ocean
572 deoxygenation on primary production in the eastern tropical North Atlantic, *Biogeosciences*,
573 12, 7467-7482, 2015.

574 MacLennan, D. N., Fernandes, P. G., and Dalen, J.: A consistent approach to definitions and
575 symbols in fisheries acoustics, *ICES Journal of Marine Science*, 59, 365-369, 2002.

576 Marxen, J., Pick, C., Oakley, T., and Burmester, T.: Occurrence of Hemocyanin in Ostracod
577 Crustaceans, *J Mol Evol*, 79, 3-11, 2014.

578 McGillicuddy, D. J., Anderson, L. A., Bates, N. R., Bibby, T., Buesseler, K. O., Carlson, C.
579 A., Davis, C. S., Ewart, C., Falkowski, P. G., and Goldthwait, S. A.: Eddy/wind interactions
580 stimulate extraordinary mid-ocean plankton blooms, *Science*, 316, 1021-1026, 2007.

581 Menkes, C. E., Kennan, S. C., Flament, P., Dandonneau, Y., Masson, S., Biessy, B., Marchal,
582 E., Eldin, G., Grelet, J., and Montel, Y.: A whirling ecosystem in the equatorial Atlantic,
583 *Geophysical Research Letters*, 29, 48-41-48-44, 2002.

584 Mills, C.: Jellyfish blooms: are populations increasing globally in response to changing ocean
585 condition?, *Hydrobiologia*, 451, 55-68, 2001.

586 Palacios, D. M., Bograd, S. J., Foley, D. G., and Schwing, F. B.: Oceanographic
587 characteristics of biological hot spots in the North Pacific: A remote sensing perspective,
588 Deep Sea Research Part II: Topical Studies in Oceanography, 53, 250-269, 2006.

589 Picheral, M.G., Stemmann, L., Karl, D.M., Iddaoud, G., Gorsky, G. The Underwater Vision
590 Profiler 5: An advanced instrument for high spatial resolution studies of particle size spectra
591 and zooplankton. Limnol Oceanogr Methods 8: 462-473. doi: 10.4319/lom.2010.8.462, 2010

592 Postel, L., da Silva, A. J., Mohrholz, V., and Lass, H.-U.: Zooplankton biomass variability off
593 Angola and Namibia investigated by a lowered ADCP and net sampling, Journal of Marine
594 Systems, 68, 143-166, 2007.

595 Prince, E. D., Luo, J. C., Goodyear, P., Hoolihan, J. P., Snodgrass, D., Orbesen, E. S., Serafy,
596 J. E., Ortiz, M., and Schirripa, M. J.: Ocean scale hypoxia based habitat compression of
597 Atlantic istiophorid billfishes, Fisheries Oceanography, 19, 448-462, 2010.

598 Ressler, P. H.: Acoustic backscatter measurements with a 153kHz ADCP in the northeastern
599 Gulf of Mexico: determination of dominant zooplankton and micronekton scatterers, Deep
600 Sea Research Part I: Oceanographic Research Papers, 49, 2035-2051, 2002.

601 Rutherford Jr, L. D. Thuesen, E.V.: Metabolic performance and survival of medusae in
602 estuarine hypoxia, Marine Ecology Progress Series, 294, 189-200, 2005.

603 Saltzman, J. and Wishner, K. F.: Zooplankton ecology in the eastern tropical Pacific oxygen
604 minimum zone above a seamount: 2. Vertical distribution of copepods, Deep Sea Research
605 Part I: Oceanographic Research Papers, 44, 931-954, 1997.

606 Schütte, F., Brandt, P., and Karstensen, J.: Occurrence and characteristics of mesoscale eddies
607 in the tropical northeast Atlantic Ocean, Ocean Science Discussions, 12, 3043-3097, 2015.

608 Schütte, F., Karstensen, J., Krahnmann, G., Fiedler, B., Brandt, P., Visbeck, M., and
609 Körtzinger, A.: Characterization of “dead-zone eddies” in the tropical North Atlantic Ocean,
610 Biogeosciences Discuss., 2016.

611 Séguin, F.: Zooplankton community near the island of São Vicente in the Cape Verde
612 archipelago: insight on pelagic copepod respiration, MSc Thesis, University of Bremen, 77
613 pp., 2010.

614 Stanton, T. K., Wiebe, P. H., Chu, D., Benfield, M. C., Scanlon, L., Martin, L., and Eastwood,
615 R. L.: On acoustic estimates of zooplankton biomass, *ICES Journal of Marine Science*, 51,
616 505-512, 1994.

617 Stramma, L., Johnson, G. C., Sprintall, J., and Mohrholz, V.: Expanding Oxygen-Minimum
618 Zones in the Tropical Oceans, *Science*, 320, 655-658, 2008.

619 Stramma, L., M. Visbeck, P. Brandt, T. Tanhua, and D. Wallace: Deoxygenation in the
620 oxygen minimum zone of the eastern tropical North Atlantic, *Geophys. Res. Lett.*, 36,
621 L20607, doi:10.1029/2009GL039593, 2009.

622 Stramma, L., Prince, E. D., Schmidtko, S., Luo, J., Hoolihan, J. P., Visbeck, M., Wallace, D.
623 W., Brandt, P., and Körtzinger, A.: Expansion of oxygen minimum zones may reduce
624 available habitat for tropical pelagic fishes, *Nature Climate Change*, 2, 33-37, 2012.

625 Stramma, L., Bange, H. W., Czeschel, R., Lorenzo, A., and Frank, M.: On the role of
626 mesoscale eddies for the biological productivity and biogeochemistry in the eastern tropical
627 Pacific Ocean off Peru, *Biogeosciences*, 10, 7293-7306, 2013.

628 Teixeira, M. C., Budd, M. P., and Strayer, D. L.: Responses of epiphytic aquatic
629 macroinvertebrates to hypoxia, *Inland Waters*, 5, 75-80, 2014.

630 Teuber, L., Schukat, A., Hagen, W., and Auel, H.: Distribution and ecophysiology of calanoid
631 copepods in relation to the oxygen minimum zone in the eastern tropical Atlantic, *PloS one*,
632 8, e77590, doi: 10.1371/journal.pone.0077590, 2013.

633 Tew Kai, E. and Marsac, F.: Influence of mesoscale eddies on spatial structuring of top
634 predators' communities in the Mozambique Channel, *Progress in Oceanography*, 86, 214-223,
635 2010.

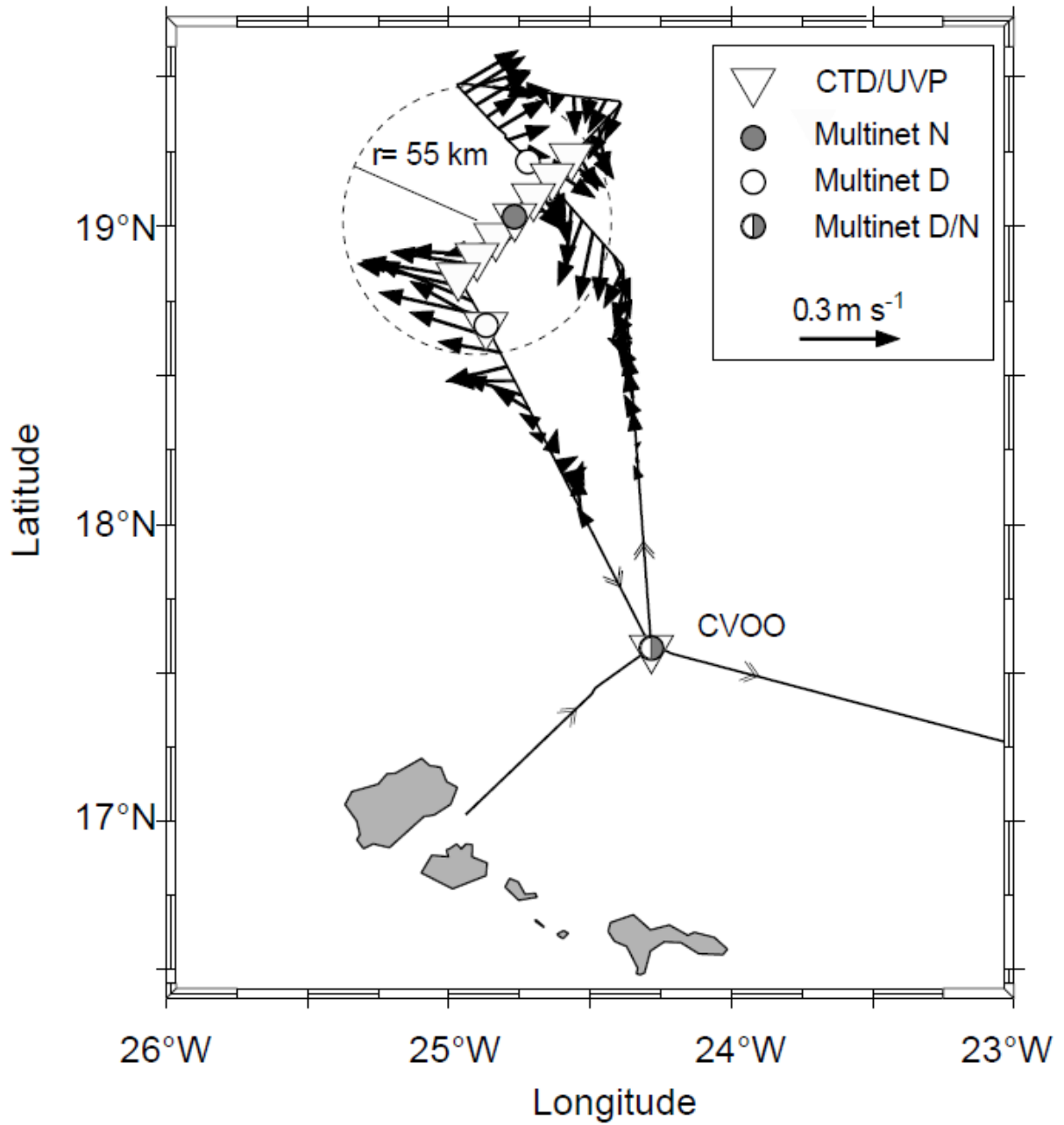
636 Thuesen, E. V. and Childress, J. J.: Metabolic rates, enzyme activities and chemical
637 compositions of some deep-sea pelagic worms, particularly *Nectonemertes mirabilis*
638 (*Nemertea*; *Hoploneuridae*) and *Poecobius meseres* (*Annelida*; *Polychaeta*), *Deep Sea*
639 *Research Part I: Oceanographic Research Papers*, 40, 937-951, 1993.

640 Thuesen, E. V., Rutherford, L. D., Brommer, P. L., Garrison, K., Gutowska, M. A., and
641 Towanda, T.: Intragel oxygen promotes hypoxia tolerance of scyphomedusae, *Journal of*
642 *Experimental Biology*, 208, 2475-2482, 2005.

- 643 Tremblay, N., Zenteno-Savín, T., Gómez-Gutiérrez, J., and Maeda-Martínez, A. N.:
644 Migrating to the Oxygen Minimum Layer: Euphausiids. In: *Oxidative Stress in Aquatic*
645 *Ecosystems*, John Wiley and Sons, Ltd, pp. 89-98, doi: 10.1002/9781444345988.ch6, 2011.
- 646 Wiebe, P. and Flierl, G.: Euphausiid invasion/dispersal in Gulf Stream cold-core rings,
647 *Australian Journal of Marine and Freshwater Research*, 34, 625-652, 1983.

648

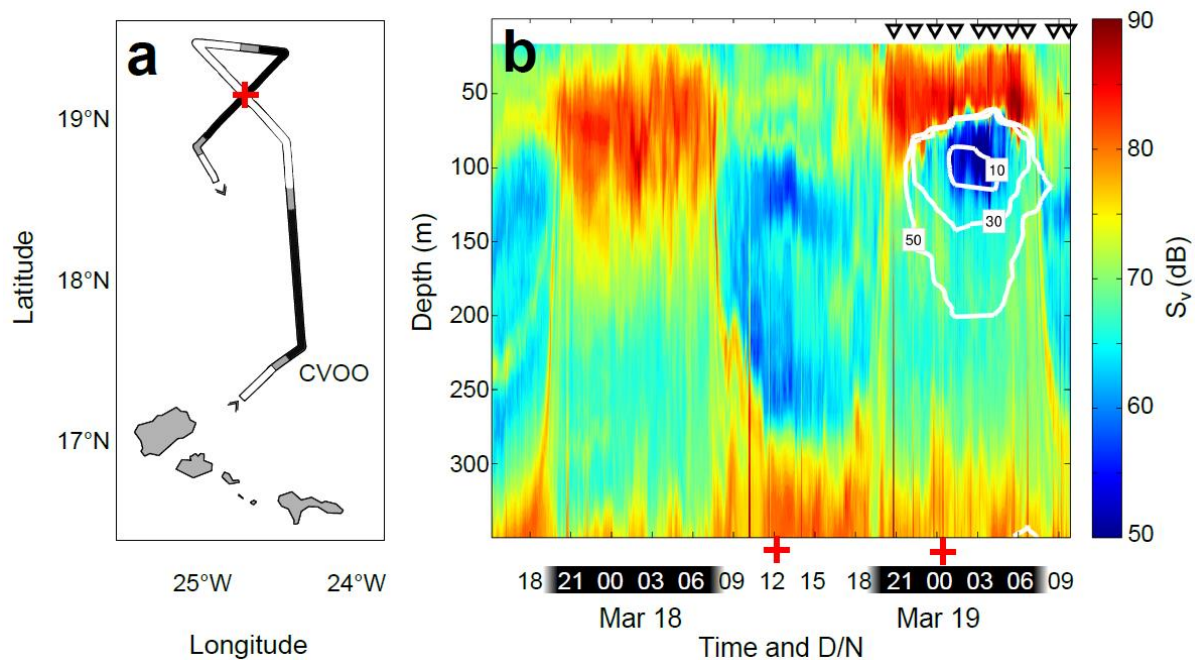
649 **Figures**



650

651 Figure 1. Cruise track (M105, only shown from Mar 17 to Mar 20, 2014) with horizontal
652 current velocities (arrows) and CTD/UVP sampling positions (triangles) as well as multinet
653 stations (gray circles = night, empty circles = day). Large dashed circle indicates the
654 estimated radius of the eddy based upon current structure.

655



656

657 Figure 2. Cruise track with indicated day- and nighttime hours (panel a, red cross indicates
 658 intersection of day- and nighttime section) and Shipboard Acoustic Doppler Current Profiler
 659 (ADCP) mean volume backscatter S_v at 75 kHz (panel b, red crosses indicate the two profiles
 660 obtained at the intersection). White contour lines indicate oxygen concentrations interpolated
 661 from CTD profiles (triangles denote CTD stations).

662

663

664

665

666

667

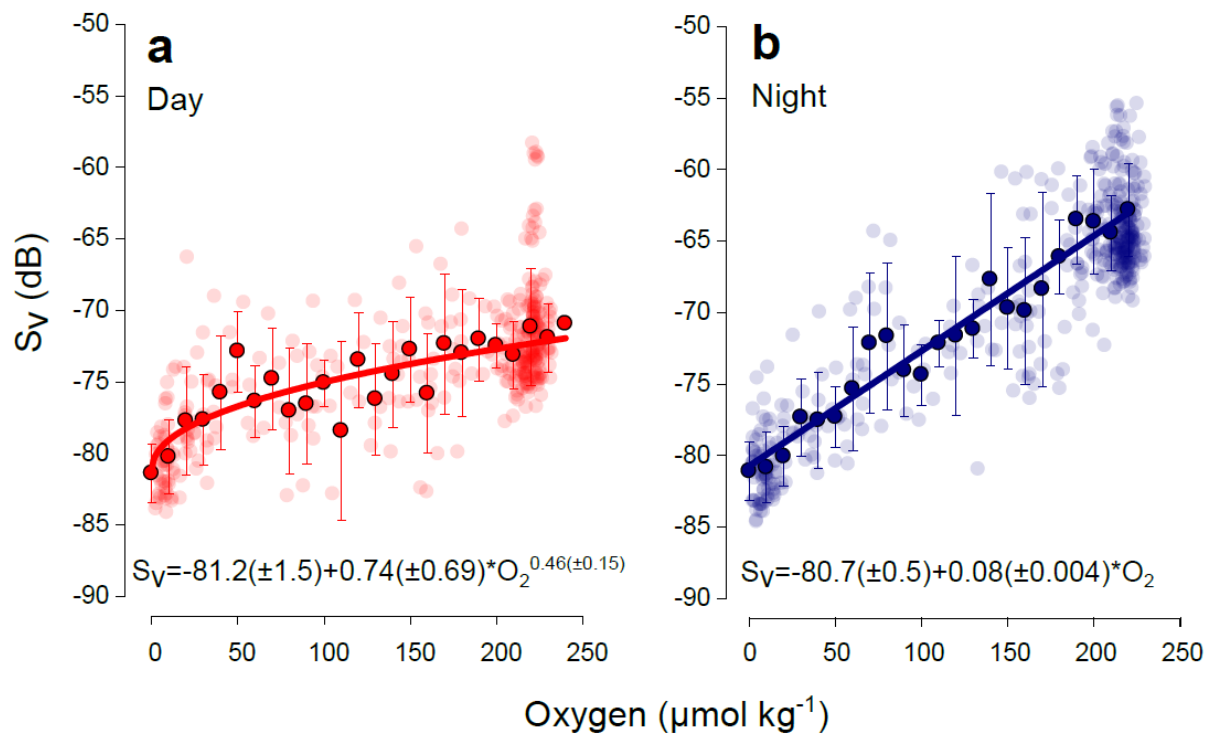
668

669

670

671

672



673

674 Figure 3. Moored ADCP (300 kHz, matched to depth of moored oxygen sensor,
 675 approximately 50 m) mean volume backscatter S_v (dB) as a function of oxygen concentration
 676 ($\mu\text{mol O}_2 \text{ kg}^{-1}$) during daytime (a) and nighttime hours (b). Higher S_v indicates a higher
 677 biomass of zooplankton and nekton. Transparent symbols are 1.5 hourly data, filled symbols
 678 are mean values ($\pm\text{SD}$) for $10 \mu\text{mol O}_2 \text{ kg}^{-1}$ bins. Data are from Jan 1 to Mar 14, 2010.

679

680

681

682

683

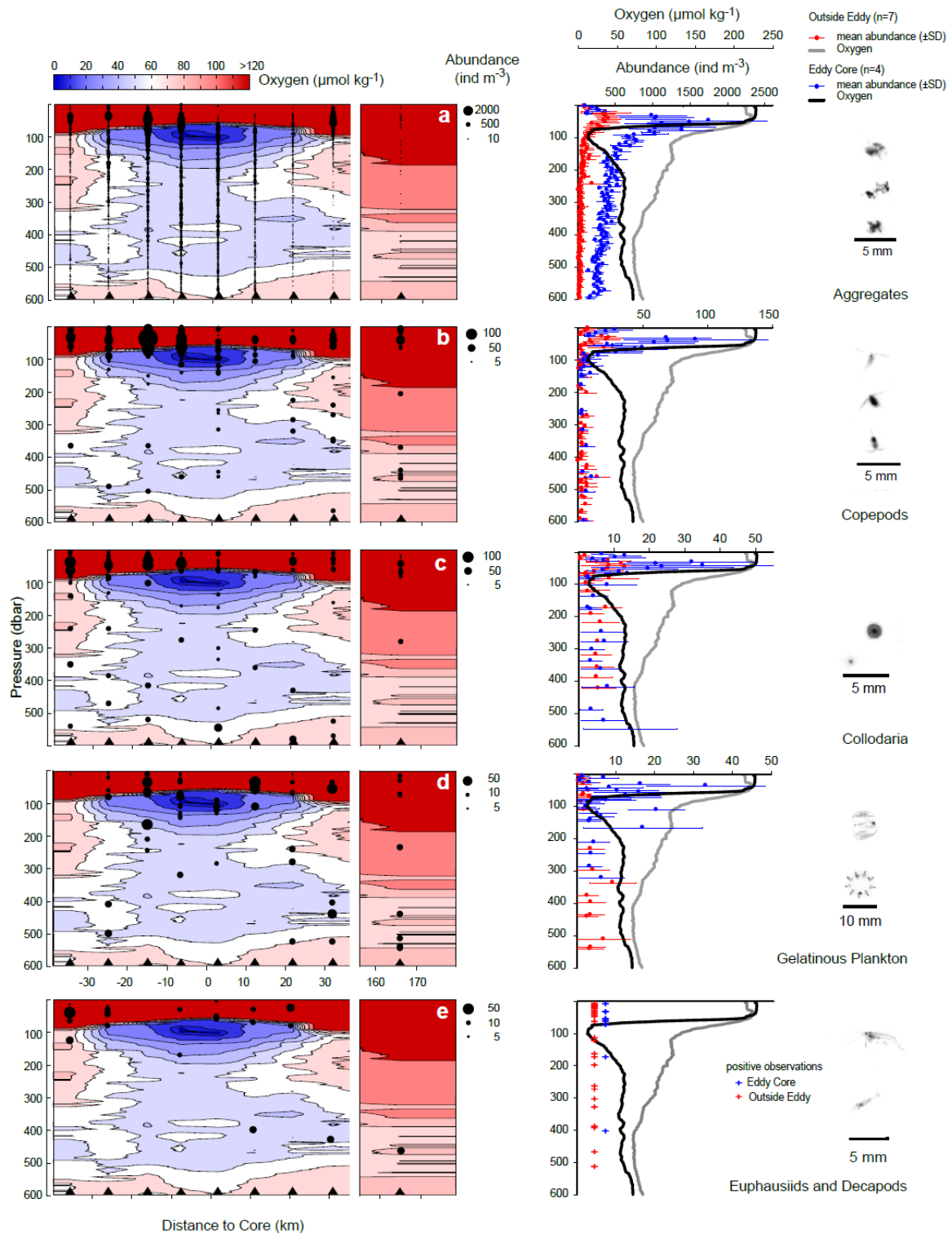
684

685

686

687

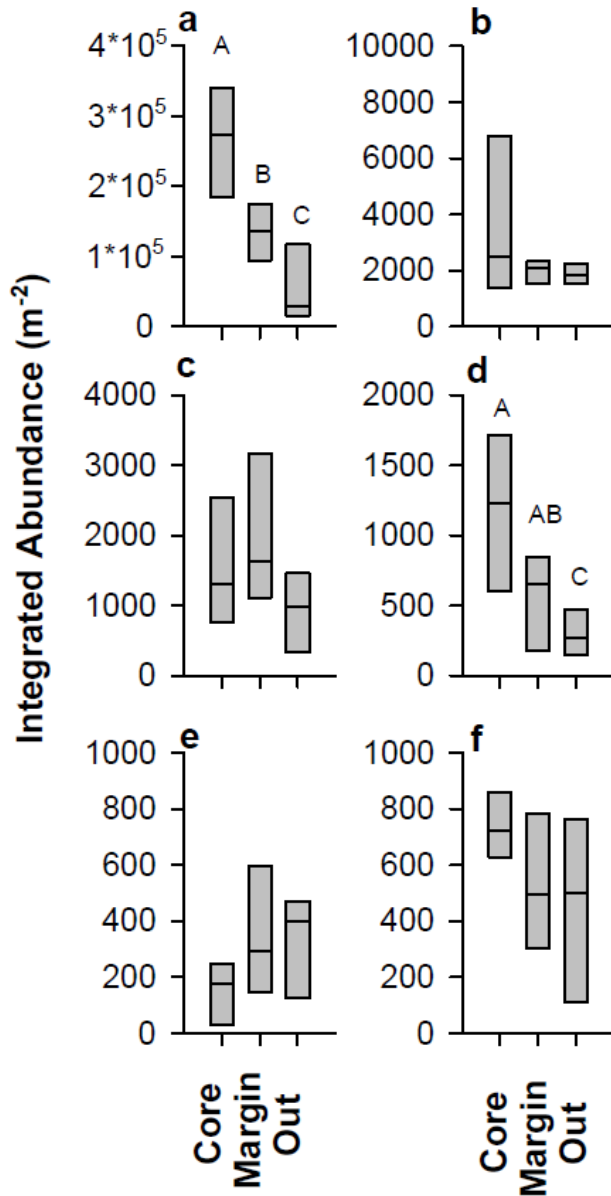
688



689

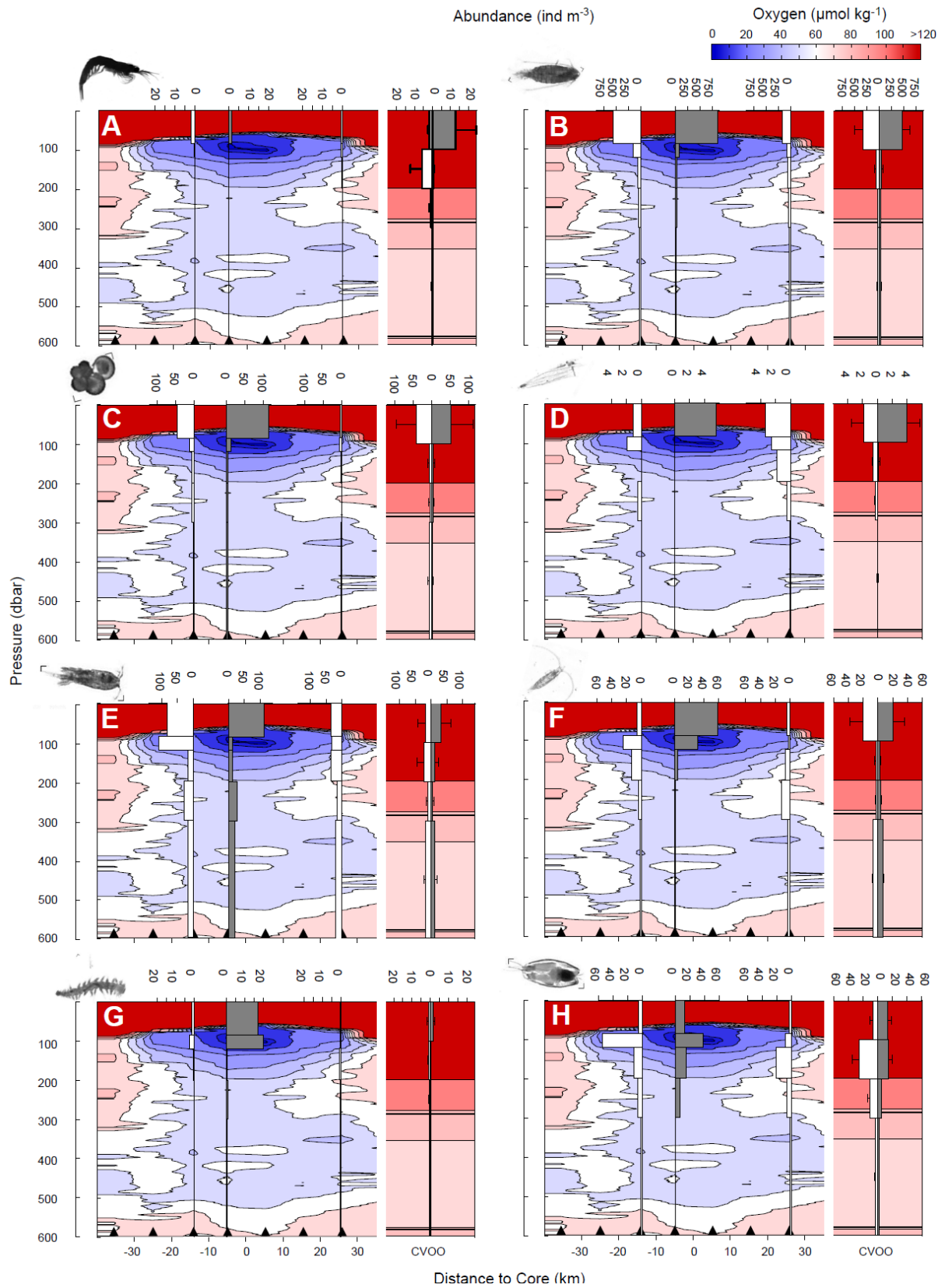
690 Figure 4. Left column shows oxygen contours ($\mu\text{mol O}_2 \text{ kg}^{-1}$) across the eddy (from NE to
 691 SW) with superimposed bubble plots of UVP-based abundance (individuals m^{-3} , in 5 m depth
 692 bins) of aggregates (panel a), copepods (b), collodaria (c), gelatinous plankton (d) and
 693 “shrimp-like” organisms (euphausiids and decapods, e). Note break in distance axis on

694 section panels. Triangles denote CTD/UVP stations. Middle column are profiles of mean
 695 (\pm SD) abundance within the eddy core (n=4) and at the CVOO station (n=7) along with mean
 696 oxygen profiles with the exception of euphausiids and decapods (e), where “+” denotes
 697 positive observations. For better visibility at low values, data with mean abundance = 0 are
 698 omitted. Right column shows representative images of the respective category.



699

700 Figure 5. UVP5-derived integrated abundance (m^{-2} , upper 600 m) of large aggregates (>500
 701 μm , panel a), copepods (b), collodaria (c), gelatinous plankton (d), shrimp-like micronekton
 702 (euphausiids/decapods, e) and phaeodaria (f) in the eddy core (n=4 profiles), eddy margin
 703 (n=4) and outside of the eddy (n=7). Different letters denote significant differences.



704

705 Figure 6. Oxygen contours (μmol O₂ kg⁻¹) across the eddy (from NE to SW) with
 706 superimposed bar plots of multinet-based abundance (individuals m⁻³) of euphausiids (a),

707 calanoid copepods (b), foraminifera (c), siphonophores (d), *Oncaea* sp. (e), eucalanid
708 copepods (f), polychaetes (g), and ostracods (h). White and grey bars indicate daylight and
709 nighttime hauls, respectively. Triangles denote CTD stations used for the O₂ section. For the
710 CVOO station (“outside eddy” situation), the mean (+SD) of four D/N samplings is shown
711 and the distance to core is not calculated because data were combined from different cruises.
712 Representative images are shown next to the respective category panel.